Published in final edited form as:
Chem Biol. 2011 August 26; 18(8): 1021–1031. doi:10.1016/j.chembiol.2011.07.015.

Analysis of the Ketosynthase-Chain Length Factor Heterodimer from the Fredericamycin Polyketide Synthase

Ping-Hui Szu[§], **Sridhar Govindarajan**[†], **Michael J. Meehan**[¶], **Abhirup Das**[§], **Don D. Nguyen**[¶], **Pieter C. Dorrestein**[¶], **Jeremy Minshull**[†], and **Chaitan Khosla**[§,±,¥,*]

[§]Department of Chemistry, Stanford University, Stanford, California 94305-5025

[±]Department of Chemical Engineering, Stanford University, Stanford, California 94305-5025

[¥]Department of Biochemistry, Stanford University, Stanford, California 94305-5025

[†]DNA2.0 Inc., 1430 O'Brien Drive, Suite E, Menlo Park, CA 94025

[¶]Skaggs School of Pharmacy and Pharmaceutical Sciences and Departments of Pharmacology, Chemistry and Biochemistry, University of California, San Diego, CA 92093

SUMMARY

The pentadecaketide fredericamycin has the longest carbon chain backbone among polycyclic aromatic polyketide antibiotics whose biosynthetic genes have been sequenced. This backbone is synthesized by the bimodular *fdm* polyketide synthase (PKS). The initiation module is thought to synthesize a C_6 intermediate that is then transferred onto the elongation PKS module, which extends it into a C_{30} poly-β-ketoacyl product. Here we demonstrate that the bimodular *fdm* PKS as well as its elongation module alone synthesize undecaketides and dodecaketides. Thus, unlike other homologues, the *fdm* ketosynthase – chain length factor (KS-CLF) heterodimer does not exclusively control the backbone length of its natural product. Using sequence- and structure-based approaches, 48 multiple mutants of the CLF were engineered and analyzed. Unexpectedly, the I134F mutant was unable to turn over, but could initiate and at least partially elongate the polyketide chain. This unprecedented mutant suggests that the KS-CLF heterodimer harbors an as yet uncharacterized chain termination mechanism. Together, our findings reveal fundamental mechanistic differences between the *fdm* PKS and its well-studied homologues.

INTRODUCTION

Polyketide synthases (PKSs) are a large family of multienzyme assemblies that catalyze the biosynthesis of structurally diverse and medicinally important natural products (O'Hagan, 1991; Rawlings, 1999; Staunton and Weissman, 2001). In analogy with the evolutionarily related fatty acid synthases, they are classified into Type I and Type II PKSs (Hopwood and Sherman, 1990; Smith and Tsai, 2007). The latter sub-class of PKSs, which resemble bacterial and plant fatty acid synthases, play a defining role in the biosynthesis of many polycyclic aromatic antibiotics produced by the actinomycetes (Das and Khosla, 2009; Hertweck et al., 2007). They invariably harbor a minimal PKS module comprised of a ketosynthase (KS), a chain length factor (CLF), an acyl carrier protein (ACP), and a

[*]To whom correspondence should be addressed. khosla@stanford.edu.

malonyl-CoA:ACP transacylase (MAT, usually from the housekeeping fatty acid synthase in the bacterium). Collectively, these proteins catalyze the formation of a poly-β-ketoacyl-ACP chain of defined length. In addition, some Type II PKSs also have an initiation module that catalyzes the first one or two cycles of polyketide chain growth (reviewed in Das and Khosla, 2009).

The heterodimeric KS-CLF is central to the activity of Type II PKSs, not only because it catalyzes chain elongation but also because it controls product length. In well-studied examples such as the actinorhodin and tetracenomycin PKS, the CLF subunit has been shown to be necessary and sufficient for dictating polyketide chain length (McDaniel et al., 1993; Tang et al., 2003). Because chemical diversity of the resulting natural products correlates with chain length (Shen et al., 1999), we sought to investigate the KS-CLF heterodimer from the fredericamycin A (**1**, Figure 1) biosynthetic gene cluster (Wendt-Pienkowski et al., 2005). With a C_{30} backbone, this antitumor aromatic polyketide has the longest known carbon chain length. In earlier work (Das et al., 2010), we showed that the initiation module of the fredericamycin (*fdm*) PKS catalyzes the synthesis of an ACP-linked C_6 intermediate. The goal of the current study was therefore to understand how the *fdm* KS-CLF catalyzes chain elongation to its full length. To do so, we functionally reconstituted it in a heterologous host as well as *in vitro*. Using sequence- and structure-based methods, we designed and expressed a set of 48 multiple mutants of the CLF gene, and compared the properties of the resulting KS-CLF heterodimers to those of the wild-type enzyme. Our findings reveal several fundamentally novel aspects of how the *fdm* KS-CLF controls chain length.

RESULTS

Reconstitution and analysis of the *fdm* PKS in *S. coelicolor* CH999

As a first step in our analysis of the *fdm* KS-CLF, we exploited the engineered host-vector system *Streptomyces coelicolor* CH999/pRM5 (McDaniel et al., 1993). Plasmid pAD201 was constructed harboring the KS-CLF (*fdmFG*) and ACP (*fdmH*) genes. We also inserted the *fdmW* phosphopantetheinyl transferase gene on this plasmid, because previous studies had demonstrated that, absent this enzyme, the *fdm* ACP is inactive in the native host *S. griseus* (Wendt-Pienkowski et al., 2005) as well as *S. coelicolor* CH999 (Das et al., 2010). Plasmid pAD201 was introduced via transformation into *S. coelicolor* CH999 along with a secondary plasmid pBOOST*, which amplifies the copy number of the cloned PKS genes, thereby enhancing protein expression as well as product formation (Hu et al., 2003). Two previously characterized undecaketides (TW94b and TW94c, Fig. 1) and one known dodecaketide (TW94d, Fig. 1) were isolated as the major products from an ethyl acetate: methanol (90:10) extract of this recombinant strain. TW94b (**2**), TW94c (**3**) and TW94d (**4**) were produced in a 2:1:2 ratio. Their identities were verified by ^{1}H and ^{13}C NMR in comparison to authentic standards (Yu et al., 1998). Two conclusions can be drawn from this finding. First, in the absence of the initiation module, the minimal *fdm* PKS catalyzes chain initiation via decarboxylative priming of a malonyl extender unit. Second, and more importantly, the minimal *fdm* PKS intrinsically appears to be a dodecaketide synthase. (The concomitant biosynthesis of undecaketides TW94b and TW94c along with the dodecaketide TW94d has precedence in a number of spore pigment PKSs, such as the *whiE* PKS (Yu et al., 1998).)

To interrogate the influence of the initiation module on the minimal PKS, the *fdmS*, *fdmC*, and *fdmO* genes were inserted onto plasmid pAD201, yielding plasmid pAD210. The resulting transformant, *S. coelicolor* CH999/pAD210/pBOOST*, synthesized a new product AD210a (**5**, Fig. 1) with an observed molecular mass of 439 and 441 (in negative and positive ionization modes, respectively) by ESI-MS. High resolution ESI-MS analysis

yielded a molecular formula of $C_{24}H_{24}O_8Na$ (calcd. 463.1361, observed 463.1369). The structure of AD210a was solved by ^1H and ^{13}C NMR spectroscopic analysis as well as HSQC, HMBC and COSY NMR experiments (Table 1), and revealed that, even in the presence of the initiation module, the *fdm* KS-CLF preferentially synthesizes carbon chain backbones up to 24 carbon atoms in length.

Purification and *in vitro* reconstitution of the *fdm* minimal PKS

The His_6-tagged holo-ACP and KS-CLF heterodimer from the *fdm* minimal PKS were individually expressed and purified to homogeneity (Fig. 2A, lanes 3 and 6, respectively). (The KS and the His_6-CLF have virtually identical molecular masses, and cannot be resolved on SDS-PAGE.) Whereas the holo-ACP was produced in *E. coli* BAP1, the KS-CLF could only be functionally expressed in *S. coelicolor* CH999. The MAT from *S. coelicolor* was expressed in *E. coli* BL21(DE3). These protein preparations were incubated individually and in selected combinations with [^{14}C]-malonyl-CoA (Fig. 2B). By itself, only the MAT could be labeled (lane 2). When incubated with the MAT and [^{14}C]-malonyl-CoA, the holo-ACP was also labeled (lane 4). Weak labeling of the KS-CLF and the holo-ACP was observed in the absence of the MAT (lane 5); the precise reason for this observation was not investigated. When [^{14}C]-malonyl-CoA was added to the complete minimal PKS, both the KS and the ACP were strongly labeled (lane 6), consistent with the expectation that oligoketides with higher specific radioactivity than malonyl-CoA are attached to their active sites. Taken together, these radio-SDS-PAGE results support the established model for minimal PKS activity, in which the MAT supplies malonyl units to the ACP, whereas polyketide biosynthesis involves back-and-forth transfer of the growing chain between the KS and the ACP.

To verify the ability of the reconstituted *fdm* minimal PKS to turn over, a radio-TLC (thin layer chromatography) assay was performed (Fig. 2D). In lane 2, the minimal PKS is observed to convert malonyl-CoA into polyketide products of unconfirmed structure. Notwithstanding repeated attempts on different types of mass spectrometers, we were unable to verify the identity of the products synthesized *in vitro* as TW93b, TW93c or TW93d, the expected undeca- or dodeca-ketide products of the PKS (Yu et al., 1998). Nonetheless, two observations support the assumption that the observed radiolabeled products are polyketides synthesized by the *fdm* minimal PKS. First, omission of the KS-CLF resulted in complete loss of activity (Fig. 2D, lane 3). Second, pre-incubation of the KS-CLF with the irreversible inhibitor, cerulenin, also abolished product formation (Fig. 2D, lane 1). Kinetic measurements showed that the minimal PKS turned over with a V_{max} of 0.27 μM/min, as judged by the rate of formation of the polyketide products observed in Fig. 2D, lane 2. This corresponds to a k_{cat} of 0.03 min^{-1} (referenced to the KS concentration), a comparable value to the turnover number of the *act* minimal PKS (Carreras and Khosla, 1998).

Given our inability to unambiguously identify the released product(s) of the *fdm* minimal PKS in vitro, we used electrospray ionization Fourier-Transform Mass Spectrometry (FT-MS) to verify its catalytic activity and to characterize the ACP-bound intermediates. Recently, a 4′-phosphopantetheine (PPant) ejection assay (Fig. 3A) has been developed that allows the masses of ACP-bound substrates and intermediates to be determined (Dorrestein and Kelleher, 2006; Meluzzi et al., 2008). The reaction mixture containing malonyl-CoA, holo-ACP, MAT, and the KS-CLF was incubated at room temperature for 30 min, following which the PPant ejection assay was performed. As seen in Figure 3B (see also MS^3 analysis in Figs. S1-S7, Supplementary Information), the predominant PPant ejection peaks corresponded to a tetraketide, a pentaketide, a cyclized tetraketide, and a cyclized pentaketide. Whereas this data does not allow us to verify the longest chain length attainable by the *fdm* minimal PKS, it confirms that the reconstituted system is catalytically active.

Design, synthesis and characterization of an *fdm* CLF mutant library

A major challenge for structure-function analysis or engineering of the *fdm* CLF (or any other CLF) is the lack of a high-throughput assay that is adequately sensitive to polyketide product characteristics. To mitigate this limitation, we used a synthetic gene approach to construct a modest library of 48 *fdm* CLF mutants. Mutants were designed via a combination of sequence and structure-based approaches, as well as available literature data. Specifically, the amino acid sequences of 31 CLF homologues were aligned using ClustalW (Thompson et al., 1994) (Fig. S8). Two types of scores were assigned to each position in the alignment (Minshull et al., 2005). The first score, termed “alternate conservation”, identifies relatively conserved residues whose identity correlates with chain length specificity of the PKS. Namely, PKSs producing shorter polyketide backbones share a conserved residue at this position, while those that synthesize longer chains share an alternative conserved residue. A higher alternate conservation score suggests that an amino acid change at this position has greater potential to influence chain length. The second score, termed “entropy”, reflects the chemical diversity of amino acids at a particular position in the sequence alignment, and is calculated with reference to the Dayhoff substitution matrix. A more conserved residue has a higher entropy score. Twenty residues with the highest alternate conservation scores were targeted in the first set of 24 variants, whereas fifteen substitutions selected on the basis of entropy scores were combined with five substitutions identified from previous analyses of the actinorhodin CLF (Keatinge-Clay et al., 2004; Tang et al., 2003) to design the second set of 24 variants. Because each variant harbored multiple mutations relative to the wild-type *fdm* CLF, each substitution was programmed to occur at the same frequency (i.e., 5 or 6 times). Moreover, individual mutations in a given variant were randomly combined. Thus, the variants were designed to maximize the number of different pairs of substitutions in the full set of variants. The complete set of variants is defined in Table 2A.

The product profiles of the 48 variants are summarized in Table 2B. Twelve variants (527, 532, 533, 540, 543, 544, 547, 549, 550, 557, 561, and 564) did not produce TW94b, TW94c, or TW94d. The inactivity of variant 533, which harbors D18G, F77L, Y121W, G129S, and V326A mutations, could not be exclusively ascribed to a single modification, because each mutation was also found in other biosynthetically competent variants. Radio-SDS-PAGE analysis of the corresponding purified KS-CLF confirmed that its inability to be labeled in the presence of MAT, holo-ACP and [^{14}C]-malonyl-CoA (data not shown). Further analysis of variant 533 was not undertaken, as its phenotype was likely due to the combined effect of multiple residues.

Variants 527, 532, 540, 543, and 544, whose designs were based on the alternate conservation score, all harbored the I134F mutation, whereas variants 547, 549, 550, 557, 561, and 564, whose designs were based on the entropy score, shared the G113T mutation. Because both sets of variants exhibited a null phenotype *in vivo*, the KS-CLF heterodimer from a representative variant of each set was purified. The G113T-harboring mutant was not labeled under any circumstance (data not shown); however, the I134F-harboring mutant showed interesting characteristics. To unambiguously assign the observed properties to the I134 residue, we first constructed and expressed a mutant CLF harboring a single change (I134F). The resulting transformant *S. coelicolor* CH999/pAD201-I134F/pBOOST* produced no detectable polyketide metabolite.

In vitro analysis of the I134F mutant of the *fdm* CLF

Using a similar protocol to the wild-type enzyme purification procedure, the KS-CLF heterodimer harboring the I134F mutation in the CLF was purified to homogeneity (Figure 2A, lane 5). As predicted from the *in vivo* phenotype of this mutant, radio-TLC analysis failed to show evidence of polyketide production in the presence of MAT, holo-ACP, and

[^{14}C]-malonyl-CoA (Fig. 2E). However, an unexpected labeling pattern was observed by radio-SDS-PAGE analysis (Fig. 2C). When [^{14}C]-malonyl-CoA was incubated with MAT, holo-ACP and the mutant KS-CLF, both the ACP and the KS were strongly labeled (Fig. 2C, lane 5). The intensity of protein labeling was suggestive of the possibility that polyketide intermediates were covalently attached to the holo-ACP. To test this hypothesis, a reaction mixture containing malonyl-CoA, the holo-ACP, the MAT, and the mutant KS-CLF was incubated at room temperature for 30 min, and analyzed via FT-MS. The same ACP-bound intermediates observed in the wild-type reaction (i.e. a tetraketide, a pentaketide, a cyclized tetraketide, and a cyclized pentaketide) were also observed in the case of the I134F mutant (Fig. 3C), implying that although this mutant was unable to turn over, it could initiate and (at least partially) elongate polyketide chains.

DISCUSSION

The *fdm* PKS is a bimodular synthase that is believed to synthesize the longest known (C_{30}) polyketide backbone produced by a Type II PKS (Das et al., 2010; Wendt-Pienkowski et al., 2005). Its initiation module synthesizes a C_6 primer unit and transfers it to the elongation module (Das et al., 2010), which then presumably incorporates 12 malonyl extender units (Figure 4). In all other Type II PKSs studied thus far, chain length specificity is exclusively programmed in the KS-CLF heterodimer (reviewed in Das and Khosla, 2009). For example, investigations into the actinorhodin and benastatin PKSs have shown that the number of decarboxylative condensation cycles catalyzed by their KS-CLF heterodimers depends on the size of the primer unit (Nicholson et al., 2003; Tang et al., 2004; Xu et al., 2007; Xu et al., 2009). Our findings reported here suggest that the *fdm* KS-CLF is an exception to this rule in that it only synthesizes $C_{22} – C_{24}$ backbones instead of the expected C_{30} backbone (Figure 4). It is therefore likely that an as yet unidentified auxiliary protein encoded by the *fdm* gene cluster modifies the inherent chain length specificity of the *fdm* KS-CLF, in effect enlarging its substrate-binding pocket. Further investigations are warranted to elucidate the mechanism by which this most remarkable synthase controls product length.

Besides being of fundamental interest, the ability of the *fdm* PKS to synthesize exceptionally long poly-β-ketoacyl chains also offers an attractive starting point for the engineering of biosynthetically useful enzymes. Here we have used sequence and structure-based concepts together with machine learning algorithms and high-throughput gene synthesis to identify two important residues, I134 and G116, in the *fdm* CLF. The I134F mutant is particularly noteworthy because, to our knowledge, it is the first example of a CLF mutant that can initiate and elongate, but not terminate, polyketide chain growth. Earlier efforts to modify the substrate-binding pocket of the *act* and *tcm* CLF proteins resulted in mutants that retained the ability to turn over but had altered backbone length specificity (Tang et al., 2003). Alternatively, mutants such as G113T and variant 533 of the *fdm* CLF (reported here) are completely inactive. In contrast, the partial activity of the I134F mutant suggests that chain termination by the KS-CLF is not simply a default event that occurs when further growth of the polyketide backbone is no longer possible. A homology model of the *fdm* KS-CLF, based upon the X-ray crystal structure of the *act* KS-CLF (Keatinge-Clay et al., 2004), is shown in Figure 5. According to this model, I134 is located at the inter-subunit interface. We speculate that the I134F mutation creates a steric block in the substrate-binding channel straddling this interface. However, in contrast to earlier CLF mutants with alterations in the substrate binding channel (Tang et al., 2003), the product of the I134F mutant is not released. Therefore, chain termination must require repositioning of a full-length chain to promote its ejection from the elaborate substrate-binding pocket. Further structural and mechanistic analysis of this *fdm* PKS mutant will not only shed light on the mechanism of chain length control, but could also provide entirely new insights into the mechanism of chain termination by Type II PKSs.

SIGNIFICANCE

Type II polyketide synthases (PKSs) catalyze the biosynthesis of highly reactive poly-β-ketoacyl chains of defined length. Understanding and engineering polyketide chain length offers the opportunity to rationally manipulate the structures of many interesting antibiotics. We have harnessed a variety of approaches to study the ketosynthase – chain length factor (KS-CLF) heterodimer from the fredericamycin PKS. Although fredericamycin is derived from a C_{30} backbone, we show that its KS-CLF synthesizes products in the $C_{22} – C_{24}$ range. Thus, this heterodimeric enzyme appears unique in that its chain length specificity is considerably shorter than the backbone length of the final product. We have also identified a prototypical CLF mutant that permits chain initiation and elongation, but not termination. Further characterization of this mutant should yield fundamentally new insights into the mechanisms by which carbon chains of defined length are synthesized and released.

EXPERIMENTAL SECTION

Materials

Radiolabeled coenzyme A (CoA) substrates were from American Radiolabeled Chemicals (St. Louis, MO). All other biochemicals were from Sigma-Aldrich (St. Louis, MO). Deuterated solvents for NMR experiments were from Cambridge Isotope Laboratories (Andover, MA); all other solvents were from Fisher Scientific (Pittsburgh, PA) at highest available grade. Hi-Trap Q anion-exchange column was from GE Healthcare (Madison, WI). Precast SDS-PAGE gels were from Invitrogen (Carlsbad, CA). PCR was performed using *PfuTurbo* Hotstart polymerase (Stratagene, La Jolla, CA), and amplimers were sequence-verified prior to use. Plasmids used for cloning included pLitmus28i, pUC18 (New England Biolabs, Ipswich, MA) and pET28b (EMD Bioscience, Madison, WI). All cloning steps were performed in *E. coli* XL1-Blue (Stratagene, La Jolla, CA). Unmethylated DNA was obtained by passaging plasmids through the methylase-deficient strain *E. coli* ET12567. Protoplast preparation and PEG-assisted transformation were performed as described by Hopwood *et al* (Kieser et al., 2000). *S. coelicolor* CH999/pBOOST* (Hu et al., 2003) and *E. coli* strains BL21(DE3) or BAP1 (Pfeifer et al., 2001) were used for polyketide isolation and protein expression, respectively.

Cloning

The *fdm* PKS genes were synthesized to introduce suitable restriction sites and ribosomal binding sites. The 5′ and 3′ sequences for *fdmC*, *fdmF*, *fdmG*, *fdmH*, *fdmO*, *fdmS*, and *fdmW* were engineered as follows:

*fdmC: TCTAGA***GGAGG**AGCC*CATATG*CTCACGCCCGGCCGG-------

GGCGGGATCGCCCTGTG*ACTAGT*ggtaccgagctc*GAATTC*,

*fdmF: TCTAGA*ttaattaa**GGAGG**ACC*CATATG*ACCGCACGTGCGGTG-------

CCGAGGAGGATCGCATGA*ACTAGT*aagctt,

*fdmG: TCTAGA***GGAGG**ACC*CATATG*ACCGGGCCCGTCATC-------

GTCCTCAGATCCGTCTGA*ACTAGT*aagctt,

*fdmH: TCTAGA***GGAGG**AGCG*CATATG*AGCACCATCAGCTTC-------

CTGTGTGAGGGGGTCTG*ACTAGT*ggtaccgagctc*GAATTC*,

*fdmO: TCTAGA*B**GGAGG**AGCC*CATATG*GAACTTCGACTGGTA-------

GTCGACGGGGGTGTCTGACTAGTaagctt,

*fdmS: TCTAGA***GGAGG**AGCC*CATATG*ACTGCGATCCGGGAC-------

GTCGTCCGGCTCCCCTGACTAGTaagctt,

*fdmW: TCTAGA***GGAGG**AGCC*CATATG*CAACCTGACGACGAG-------

GTCGTCGGTGCGGCCTG*ACTAGT*ggtaccgagctc*GAATTC*.

The *fdmG* gene was amplified to introduce a His_6-tag with the following primers: *fdmG*_FP: AAT*TCTAGA***GGAGG**ACC*CATATG*CATCATCATCATCATCATACCGGGCCCGTCCA TCACCGGGGTGGGCG, and *fdmG*_RP: AGC*GAATTC*GGGG*ACTAGT*TCAGACGGCTCTGAGGACCA. The underlined sequence encodes the His_6-tag. Restriction sites are indicated in italics or in lowercase, and ribosomal binding sites are in bold. The genes *fdmF*, *fdmH*, and *fdmW* were cloned into pLitmus28i vector by *Xba*I/*Hin*dIII digestion to introduce an *Eco*RI site at the 3′ end. They were then assembled as synthetic operons in pUC18 prior to transfer into a pRM5-derived shuttle vector (McDaniel et al., 1993). The first gene in each operon was inserted between the *Xba*I and *Eco*RI sites in pUC18; subsequent genes were inserted downstream following *Spe*I/*Eco*RI digestion of the vector and *Xba*I/*Eco*RI digestion of the insert. Plasmid pAD201 was constructed by excising the complete operon by *Pac*I/*Eco*RI digestion, which was inserted between the *Pac*I/*Eco*RI sites of shuttle vector pRM5. The *fdmS*, *fdmC*, and *fdmO* genes were inserted onto plasmid pAD201 by a similar method described above, yielding plasmid pAD210.

Protein expression and purification

S. coelicolor CH999/pAD201/pBOOST* was the source of the His_6-tagged *fdm* KS-CLF. Spores suspensions of each strain were used to inoculate 4 × 1 L minimal medium (6.25% (w/v) PEG 8000, 25 mM TES, pH 7.2, 0.5% (w/v) casamino acids, 1% (w/v) glucose, 15 mM $(NH_4)_2SO_4$, 5 mM $MgSO_4$, 1.25 mM NaH_2PO_4, 1.25 mM K_2HPO_4, 926 nM $FeCl_3$, 377 nM $ZnCl_2$, 99 nM $MnCl_2$, 73 nM $CuCl_2$, 33 nM $Na_2B_4O_7$, 10 nM $(NH_4)_6Mo_7O_{24}$) containing 50 mg/L thiostrepton and 100 mg/L apramycin. Mycelia from the stationary phase cultures (about 2 days) were collected by centrifugation, and resuspended in 140 mL disruption buffer (200 mM NaH_2PO_4, pH 7.1, 200 mM NaCl, 30% (v/v) glycerol, 2.5 mM EDTA, 2 mM DTT, 1.5 mM benzamidine, 4.3 μM leupeptin, 2.9 μM pepstatin). Cells were disrupted by sonication, and the cell debris was removed by centrifugation (17,000 rpm for 30 min). DNA was precipitated by adding 0.2% polyethyleneimine (PEI), followed by centrifugation (17,000 rpm for 30 min). The KS-CLF protein was precipitated between 30 and 50% $(NH_4)_2SO_4$. Precipitated proteins were re-dissolved in 100 mM NaH_2PO_4, pH 7.4, and incubated with 2 mL Ni-NTA resin (Qiagen) for 2 h at 4 °C. The slurry was poured into a capped column, and washed with 20 mL of the first wash buffer (50 mM sodium phosphate, 300 mM NaCl, 20 mM imidazole, pH 8.0), followed by 4 mL of the second wash buffer (50 mM sodium phosphate, 300 mM NaCl, 50 mM imidazole, pH 8.0). The KS-CLF heterodimer was eluted with elution buffer (50 mM sodium phosphate, 100 mM NaCl, 250 mM imidazole, pH 8.0). Fractions containing the KS-CLF were pooled and buffer exchanged into 45 mL of buffer A (50 mM Tris•HCl, pH 8.0, 1 mM TCEP, and 10% glycerol) and loaded onto a Hi-Trap Q column pre-equilibrated with buffer A. The following gradient was applied to this column: 0% buffer B (buffer A with 500 mM NaCl) from 0 to 20 min, 10% buffer B from 20 to 25 min, 80% buffer B from 25 to 85 min, and 100% buffer B from 85 to 100 min. The target protein eluted at 48% buffer B. The eluant was concentrated, buffer exchanged into a storage buffer (100 mM NaH_2PO_4, pH 7.4, 2 mM TCEP, 2 mM EDTA, and 15% glycerol), flash-frozen with liquid nitrogen, and stored at −80 °C. The typical yield of purified *fdm* KS-CLF was 1 mg/L.

The *fdm* holo-ACP was expressed in an engineered *E. coli* strain BAP1 (Pfeifer et al., 2001) to obtain its 4′-phosphopantetheinylated form. Protein expression was induced at an OD_{600} of 0.6 with 200 μM IPTG, and allowed to proceed at 18 °C for 18 h. Cells were harvested and lysed by sonication. The protein was initially purified on Ni-NTA resin, followed by anion exchange chromatography on a Hi-Trap Q column (from 0 to 500 mM NaCl in 60 min). The proteins eluted at 200 mM NaCl. Purified protein was buffer exchanged into 100 mM sodium phosphate, 15% glycerol, pH 7.2 and stored at −80 °C. The relative ratio of the holo and apo forms of the ACP was quantified by LC-MS, and was found to be ~50% in the holo form. The typical yield of purified ACP was 12 mg/L.

The *S. coelicolor* MAT gene was expressed in *E. coli* BL21(DE3), and the MAT protein was purified as described previously (Carreras and Khosla, 1998). The typical yield of purified MAT was 15 mg/L. All protein concentrations were determined by the Bradford method with the Bio-Rad protein kit.

Detection of covalently bound protein intermediates by radio-SDS-PAGE

To investigate the enzymatic activity of PKS components *in vitro*, selected protein combinations were incubated with radiolabeled substrates and analyzed *via* radio-SDS-PAGE. For example, a PKS reaction mixture (12 μL) contained 200 mM [^{14}C]-malonyl-CoA (55 Ci/mol), 10 μM the *fdm* KS-CLF, 25 μM holo-ACP, and 1 μM MAT in a buffer containing 100 mM sodium phosphate, pH 7.3, 2 mM EDTA, 2 mM TCEP. Following incubation at room temperature for 30 min, the reaction was quenched with 6 μL of non-reducing sample buffer (0.1% bromophenol blue, 1% SDS, 40% glycerol), and loaded directly onto a 4%–12% SDS gel. Following staining, dried gels were subjected to autoradiography.

Radio-TLC analysis of PKS activity *in vitro*

This assay detects polyketides synthesized by the *fdm* minimal PKS from radiolabeled malonyl-CoA. Assays were performed at 30 °C in 30 μL of reaction buffer, as described above. Reaction mixtures contained 50 μM holo-ACP, 10 μM KS-CLF, 0.1 μM MAT, and 1 mM [^{14}C]-malonyl-CoA (55 Ci/mol). The reaction was initiated by adding [^{14}C]-malonyl-CoA, and quenched at 2 min, 4 min, 6 min, 10 min, and 20 min by adding 200 μL ethyl acetate. Each quenched mixture was vortexed and extracted with 200 μL ethyl acetate twice. The combined organic phases were evaporated to dryness and re-dissolved in 15 μL ethyl acetate. The reaction products were separated by thin-layer chromatography (TLC) using a solvent containing 99% ethyl acetate and 1% acetic acid, and quantified with a phosphoimager. Cerulenin was used at a final concentration of 1 mM.

Production, isolation, and characterization of polyketide products

For small scale cultivations, *Streptomyces* strains were grown on R5 agar plates containing 50 mg/L thiostrepton and 100 mg/L of apramycin at 30 °C for 7 days. For HPLC analysis, the pigmented agar medium from 10–12 plates was mashed and extracted with methanol/ethyl acetate (10:90). The solvent was evaporated *in vacuo*, and the residue was dissolved in methanol. The mixture was analyzed by reverse-phase HPLC outfitted with a UV-Vis detector at 280 and 410 nm, using the Apollo C_{18} column (250 mm × 4.6 mm). A linear gradient from 30% acetonitrile (MeCN) in water (0.1% TFA) to 55% MeCN in water (0.1% TFA) was used over 40 min with a flow rate of 1 mL/min.

For preparative scale studies, the above fermentation and extraction procedures were scaled up to 3–4 L of R5 agar medium. The solvent was removed *in vacuo*. The crude extract was flashed through a silica gel column using 1% acetic acid in ethyl acetate. The eluent was dried, re-dissolved in 3–4 mL methanol, and injected onto the preparative reverse-phase

HPLC column (250 mm × 22 mm, C_{18} column, Vydac). Gradients used included 10–40% MeCN in water (0.1% TFA) over 80 min or 20–60% MeCN in water (0.1% TFA) over 100 min, with a flow rate of 5 mL/min. Purified fractions were dried *in vacuo* or by lyophilization. In cases where further purification was warranted, the relevant HPLC fraction was re-dissolved in 0.5–1 mL acetone and applied to a preparative TLC plate, which was developed in a solvent system consisting of ethyl acetate and hexane with or without 1% acetic acid. ^{1}H and ^{13}C NMR spectra of purified polyketide products were recorded on Varian Inova 500. The ^{1}H NMR spectra were referenced at 2.49 ppm in DMSO-d_6 or 3.31 ppm in CD_3OD. The ^{13}C NMR spectra were referenced at 39.5 ppm in DMSO-d_6.

Synthesis of genes encoding CLF variants

High throughput gene synthesis was carried out to synthesize these variants (Villalobos et al., 2006).

Detection of covalently bound intermediates using Electrospray Ionization (ESI) Fourier-Transform Mass Spectrometry (FT-MS)

A reaction mixture (50 μL) contained 1 mM malonyl-CoA, 6.9 μM KS-CLF heterodimer, 34.7 μM holo-ACP, and 0.7 μM MAT in a buffer containing 100 mM sodium phosphate, pH 7.3, 2 mM EDTA, 2 mM TCEP. Following incubation at room temperature for 30 min, the reaction mixtures were purified using the Phenomenex C_4 column (150 mm × 4.6 mm). A linear gradient from 10% acetonitrile (MeCN) in water (0.1% TFA) to 90% MeCN in water (0.1% TFA) was used over 30 min with a flow rate of 1 mL/min. The eluent was collected as 1 mL fractions, lyophilized to dryness, and re-dissolved in an ESI solvent containing 49.5% water, 49.5% methanol, and 1% formic acid for FT-MS analysis. ESI-FT-MS analysis was performed on a Thermo Electron LTQ-FT-ICR hybrid mass spectrometer.

The HPLC fraction containing the *fdm* ACP was re-dissolved in the ESI solvent and directly introduced into the mass spectrometer with an Advion BioSciences Nanomate 100 Biversa nanospray source. The instrument was operated in positive ion mode, using an electrospray voltage between 1.35 to 1.45 kV and gas pressure of 0.35 psig. Samples were subjected to in-source fragmentation by adjusting the skimmer voltage to 75 V. In-source fragmentation allowed for ejection of the phosphopantetheine arm from the ACP, along with any acyl-intermediate bound to it. The identities of these pantetheine-bound intermediates were determined by intact exact mass analysis followed by MS/MS (MS^3) fragmentation. In order to achieve sufficient ion intensity for MS^3 identification, pantetheine ejection ions were trapped using an isolation width of 4 m/z centered on the ion of interest. MS^3 fragmentation employed the following settings: normalized collision energy of 30%, an activation Q of 0.200 to 0.230, and an activation time of 50 to 100 ms depending on the intensity of the particular pantetheine ejection ion being identified. All spectra were recorded by FT-ICR-MS with a resolution of 100,000.

Supplementary Material

Refer to Web version on PubMed Central for supplementary material.

Acknowledgments

We thank Professor Sheryl Tsai and Pouya Javidpour at UC-Irvine for assistance in generating a homology model of the *fdm* KS-CLF. This research was supported by a grant from the NIH (CA 77248 to CK).

References

Carreras CW, Khosla C. Purification and *in vitro* reconstitution of the essential protein components of an aromatic polyketide synthase. Biochemistry. 1998; 37:2084–2088. [PubMed: 9518007]

Das A, Khosla C. Biosynthesis of aromatic polyketides in bacteria. Acc Chem Res. 2009; 42:631–639. [PubMed: 19292437]

Das A, Szu PH, Fitzgerald JT, Khosla C. Mechanism and engineering of polyketide chain initiation in fredericamycin biosynthesis. J Am Chem Soc. 2010; 132:8831–8833. [PubMed: 20540492]

Dorrestein PC, Kelleher NL. Dissecting non-ribosomal and polyketide biosynthetic machineries using electrospray ionization fourier-transform mass spectrometry. Nat Prod Rep. 2006; 23:893–918. [PubMed: 17119639]

Dreier J, Khosla C. Mechanistic analysis of a Type II polyketide synthase. Role of conserved residues in the b-ketoacyl synthase-chain length factor heterodimer. Biochemistry. 2000; 39:2088–2095. [PubMed: 10684659]

Hertweck C, Luzhetskyy A, Rebets Y, Bechthold A. Type II polyketide synthases: gaining a deeper insight into enzymatic teamwork. Nat Prod Rep. 2007; 24:162–190. [PubMed: 17268612]

Hopwood DA, Sherman DH. Molecular genetics of polyketides and its comparison to fatty acid biosynthesis. Annu Rev Genet. 1990; 24:37–66. [PubMed: 2088174]

Hu Z, Hopwood DA, Hutchinson CR. Enhanced heterologous polyketide production in Streptomyces by exploiting plasmid co-integration. J Ind Microbiol Biotechnol. 2003; 30:516–522. [PubMed: 12827516]

Keatinge-Clay AT, Maltby DA, Medzihradszky KF, Khosla C, Stroud RM. An antibiotic factory caught in action. Nat Struct Mol Biol. 2004; 11:888–893. [PubMed: 15286722]

Kieser, T.; Bibb, MJ.; Buttner, MJ.; Chater, KF.; Hopwood, DA. Practical Streptomyces Genetics. Norwich: The John Innes Foundation; 2000.

McDaniel R, Ebert-Khosla S, Hopwood DA, Khosla C. Engineered biosynthesis of novel polyketides. Science. 1993; 262:1546–1550. [PubMed: 8248802]

Meluzzi D, Zheng WH, Hensler M, Nizet V, Dorrestein PC. Top-down mass spectrometry on low-resolution instruments: characterization of phosphopantetheinylated carrier domains in polyketide and non-ribosomal biosynthetic pathways. Bioorg Med Chem Lett. 2008; 18:3107–3111. [PubMed: 18006314]

Minshull J, Ness JE, Gustafsson C, Govindarajan S. Predicting enzyme function from protein sequence. Curr Opin Chem Biol. 2005; 9:202–209. [PubMed: 15811806]

Nicholson TP, Winfield C, Westcott J, Crosby J, Simpson TJ, Cox RJ. First *in vitro* directed biosynthesis of new compounds by a minimal type II polyketide synthase: evidence for the mechanism of chain length determination. Chem Comm. 2003:686–687. [PubMed: 12703773]

O'Hagan, D. The Polyketide Metabolites. Chichester, UK: Ellis Howard; 1991.

Pfeifer BA, Admiraal SJ, Gramajo H, Cane DE, Khosla C. Biosynthesis of complex polyketides in a metabolically engineered strain of *E. coli*. Science. 2001; 291:1790–1792. [PubMed: 11230695]

Rawlings BJ. Biosynthesis of polyketides (other than actinomycete macrolides). Nat Prod Rep. 1999; 16:425–484. [PubMed: 10467738]

Shen Y, Yoon P, Yu TW, Floss HG, Hopwood D, Moore BS. Ectopic expression of the minimal *whiE* polyketide synthase generates a library of aromatic polyketides of diverse sizes and shapes. Proc Natl Acad Sci USA. 1999; 96:3622–3627. [PubMed: 10097087]

Smith S, Tsai SC. The type I fatty acid and polyketide synthases: a tale of two megasynthases. Nat Prod Rep. 2007; 24:1041–1072. [PubMed: 17898897]

Staunton J, Weissman KJ. Polyketide biosynthesis: a millennium review. Nat Prod Rep. 2001; 18:380–416. [PubMed: 11548049]

Tang Y, Tsai SC, Khosla C. Polyketide chain length control by chain length factor. J Am Chem Soc. 2003; 125:12708–12709. [PubMed: 14558809]

Tang Y, Lee TS, Khosla C. Engineered biosynthesis of regioselectively modified aromatic polyketides using bimodular polyketide synthases. PLoS Biol. 2004; 2:227–238.

Thompson JD, Higgins DG, Gibson TJ. CLUSTAL W: improving the sensitivity of progressive multiple sequence alignment through sequence weighting, position-specific gap penalties and weight matrix choice. Nucleic Acids Res. 1994; 22:4673–4680. [PubMed: 7984417]

Villalobos A, Ness JE, Gustafsson C, Minshull J, Govindarajan S. Gene Designer: a synthetic biology tool for constructing artificial DNA segments. BMC Biotechnol. 2006; 7:285.

Wendt-Pienkowski E, Huang Y, Zhang J, Li B, Jiang H, Kwon H, Hutchinson CR, Shen B. Cloning, sequencing, analysis, and heterologous expression of the fredericamycin biosynthetic gene cluster from *Streptomyces griseus*. J Am Chem Soc. 2005; 127:16442–16452. [PubMed: 16305230]

Xu Z, Metsä-Ketelä M, Hertweck C. Ketosynthase III as a gateway to engineering the biosynthesis of antitumoral benastatin derivatives. J Biothenol. 2009; 140:107–113.

Xu Z, Schenk A, Hertweck C. Molecular analysis of the benastatin biosynthetic pathway and genetic engineering of altered fatty acid-polyketide hybrids. J Am Chem Soc. 2007; 129:6022–6030. [PubMed: 17439117]

Yu TW, Shen Y, McDaniel R, Floss HG, Khosla C, Hopwood DA, Moore BS. Engineered biosynthesis of novel polyketides from *Streptomyces* spore pigment polyketide synthases. J Am Chem Soc. 1998; 120:7749–7759.

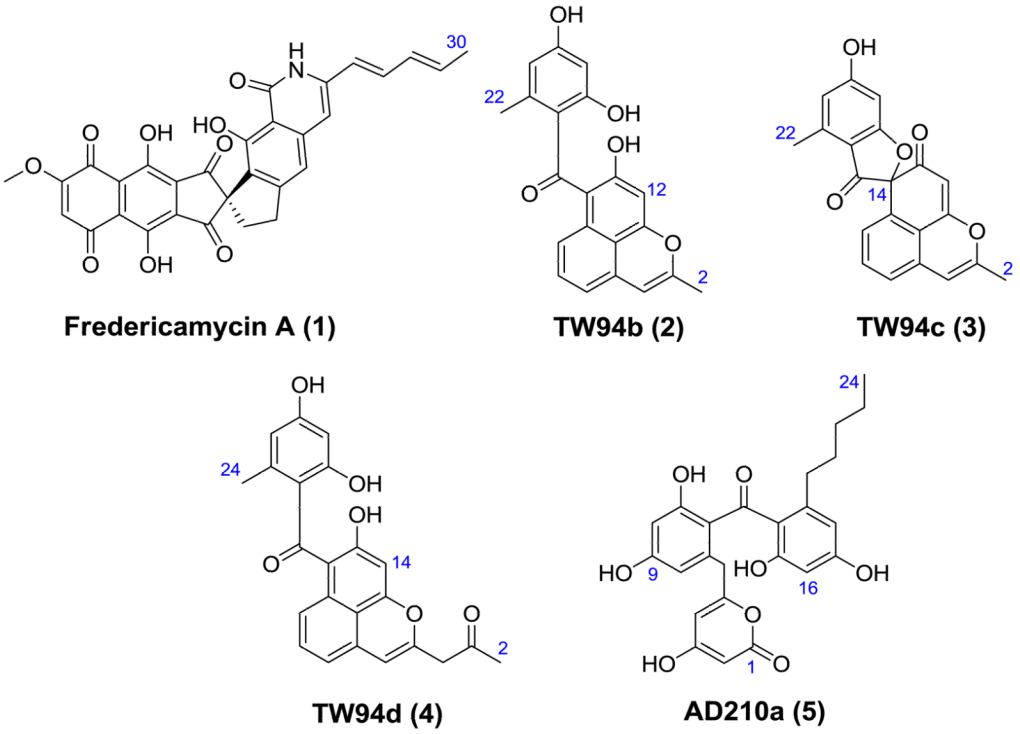

Figure 1.
Polyketides cited in this study.

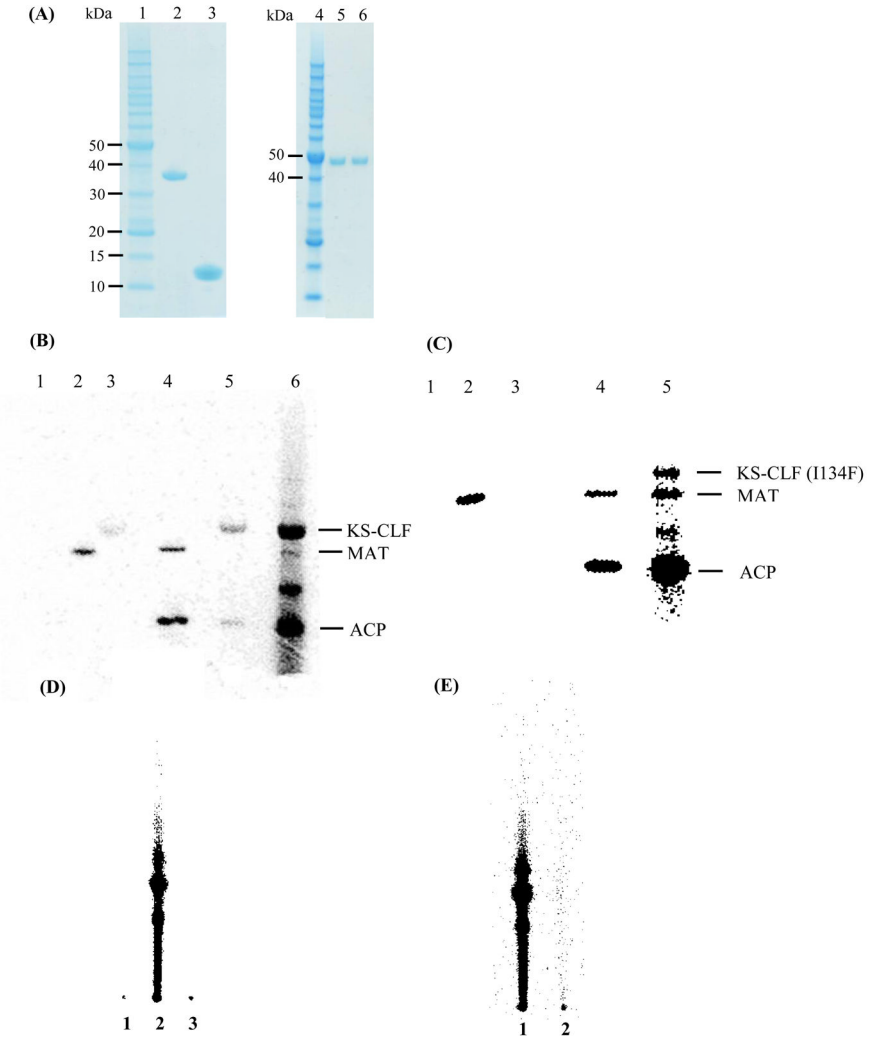

Figure 2.

(A) SDS-PAGE analysis of purified components of the *fdm* minimal PKS. Lane 1, protein molecular weight standard; lane 2, *S. coelicolor* MAT; lane 3, holo-ACP; lane 4, protein molecular weight standard; lane 5, KS-CLF I134F mutant; lane 6, wild-type KS-CLF. The two subunits have nearly identical molecular masses (44 kD and 42 kD, respectively), and therefore cannot be resolved via SDS-PAGE. **(B)** Activity of the minimal *fdm* PKS. PKS components were individually or collectively incubated with [^{14}C]-malonyl-CoA, and quenched after 30 min: Lane 1, ACP; Lane 2, MAT; Lane 3, KS-CLF; Lane 4, ACP + MAT; Lane 5, ACP + KS-CLF; Lane 6, ACP + KS-CLF + MAT. **(C)** Activity of the *fdm* PKS harboring the I134F CLF mutation. Lane 1, ACP; Lane 2, MAT; Lane 3, KS-CLF; Lane 4, ACP + MAT; Lane 5, ACP + KS-CLF + MAT. The labeled band between the MAT and ACP in lanes 6 (panel A) and 5 (panel B) has not been characterized, but has precedence in the context of other Type II PKSs (Dreier and Khosla, 2000). **(D)** Activity of purified *fdm* minimal PKS: Lane 2, Minimal PKS in the presence of [^{14}C]-malonyl-CoA (quenched at 1 h); Lane 1, Control sample pre-incubated with cerulenin for 20 min; Lane 3, Control sample lacking the KS-CLF. **(E)** Activity of the *fdm* PKS harboring the I134F CLF mutation: Lane 1, Minimal PKS in the presence of [^{14}C]-malonyl-CoA (quenched at 1 h); Lane 2, the *fdm* PKS harboring the I134F CLF mutation in the presence of [^{14}C]-malonyl-CoA (quenched at 1 h).

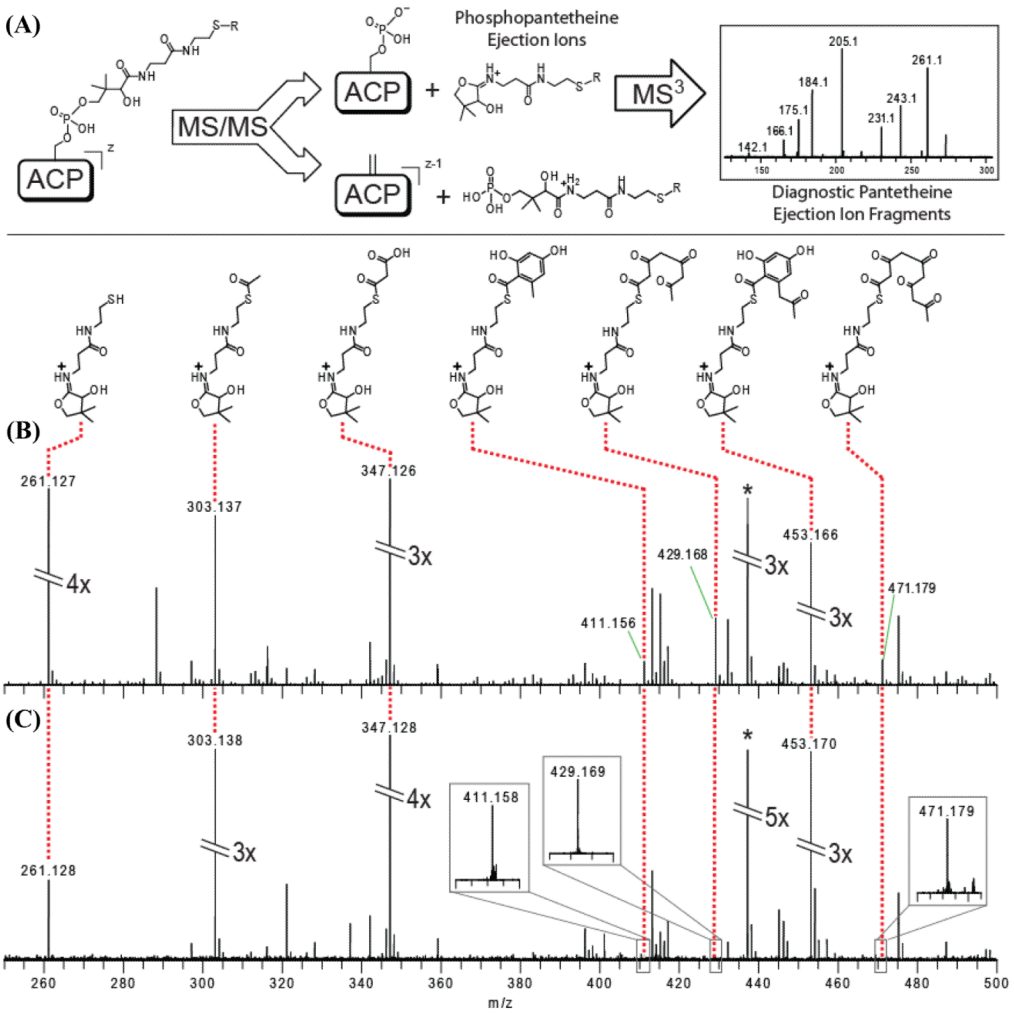

Figure 3.

FT-MS spectra of acyl-pantetheine ejection ions. **(A)** Overview of PPant ejection assay. Tandem-MS results in characteristic ejection ions bearing polyketide intermediates, which are subjected to further tandem-MS analysis to yield diagnostic fragments. In-source fragmentation of the ACP simultaneously yields multiple pantetheine ejection ions bearing different polyketide intermediates. Results from the following reactions are presented: **(B)** wild-type *fdm* PKS; and **(C)** *fdm* PKS harboring the I134F mutation in the CLF. The peak labeled (*) is a prominent, unrelated ion. Additional information for each intermediate identified by PPant ejection assay is provided in Figs S1-S7.

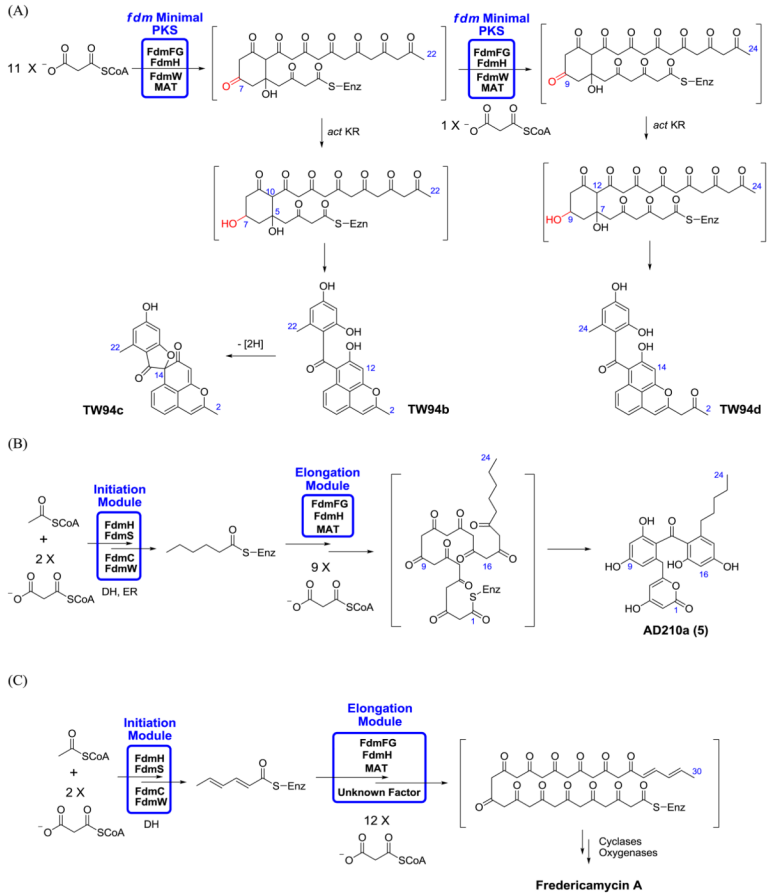

Figure 4.

(A) Proposed biosynthesis of TW94b, TW94c and TW94d by the *fdm* minimal PKS and the *act* KR in *S. coelicolor* CH999/pAD201/pBOOST*. The *act* KR is a ketoreductase from the actinorhodin biosynthetic pathway. **(B)** Proposed biosynthesis of AD210a by the bimodular *fdm* PKS in *S. coelicolor* CH999/pAD210/pBOOST*. The DH (dehydratase) and ER (enoyl reductase) involved in the initiation module are derived from the housekeeping fatty acid synthase in *S. coelicolor*. **(C)** Proposed biosynthesis of fredericamycin A in *S. griseus*.

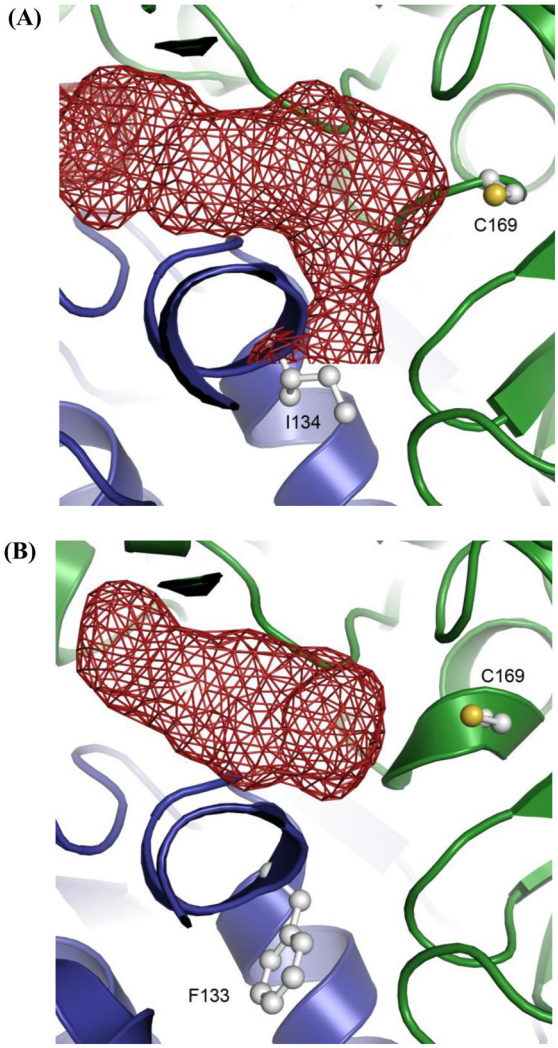

Figure 5.

Homology model of the *fdm* KS-CLF **(A)** along with the structurally characterized *act* KS-CLF **(B)**. The KS and CLF subunits are shown as green and blue ribbons, respectively. The active site of the KS (C169) and residue 134 of the *fdm* CLF (F133 is an equivalent residue in the *act* CLF) are shown in balls and sticks. Polyketide chain growth is initiated *via* decarboxylation of malonyl-ACP, followed by transfer of the resultant acetyl group onto C169 residue of the KS. The growing polyketide chain is transferred back and forth between and Cys169 residue of the KS and the pantetheinyl thiol of the ACP until it reaches full length. At this point the chain fully occupies the substrate-binding channel (shown in red), and is subsequently released.

Table 1

^{1}H and ^{13}C NMR data for AD210a (**5**). ^{1}H and ^{13}C NMR data were recorded in DMSO-d_6 (500 MHz for ^{1}H and 125 MHz for ^{13}C). Chemical shifts are reported in δ (ppm). Coupling constants are reported in Hz. Carbons are labeled according to their number in polyketide backbone.

	AD210a (5)			
no.	**^{13}C**	**^{1}H**	**Long-range ^{13}C-^{1}H HMBC correlations**	**Long-range ^{1}H -^{1}H COSY correlations**
1	160.5			
2	88.1	5.13 (*d*, *J* = 1.7, 1H)	C3, C4, C15	H4
3	170.2			
4	100.7	5.56 (*d*, *J* = 1.7, 1H)	C2, C3, C10, C20	H2
5	159.0			
6	36.9	3.51 (*s*, 2H)	C4, C7, C8, C11	
7	136.9			
8	119.1	6.21 (*d*, *J* = 1.8, 1H)	C6, C10, C11	H10
9	160.5			
10	100.1	6.08 (*d*, *J* = 1.8, 1H)	C9, C12	H8
11	164.7			
12	108.3			
13	199.7			
14	110.1			
15	163.5			
16	108.4	6.07 (*d*, *J* = 3.6, 1H)	C15, C18, C21	H18
17	160.2			
18	108.3	6.16 (*d*, *J* = 3.6, 1H)	C8, C16, C17, C20	H16
19	144.7			
20	33.1	2.19 (*t*, *J* = 6.5, 2H)	C12, C19, C21	H21
21	31.4	1.21 (*p*, *J* = 5.9, 6.5, 2H)	C20, C22, C23	H20, H22
22	30.3	1.14 (*m*, 2H)	C20, C21, C23	H21, H23
23	21.8	1.04 (*m*, 2H)	C21, C22, C24	H22, H24
24	13.9	0.78 (*t*, *J* = 5.75, 3H)	C21, C22, C23	H23

Table 2

(A) List of the variants with their corresponding mutations. Variant numbers are listed in the 1st column, and the mutations harbored by them are listed the corresponding row. A “1” in a given cell (highlighted in purple for enhanced identification) indicates that the mutation was incorporated into that variant. See also Figure S8.
(B) *In vivo* product profile of *fdm* CLF variants. Set 1 includes variants whose design was based on high “alternate conservation” scores, whereas Set 2 includes variants designed based on “entropy” scores. For details, see text.

(A)

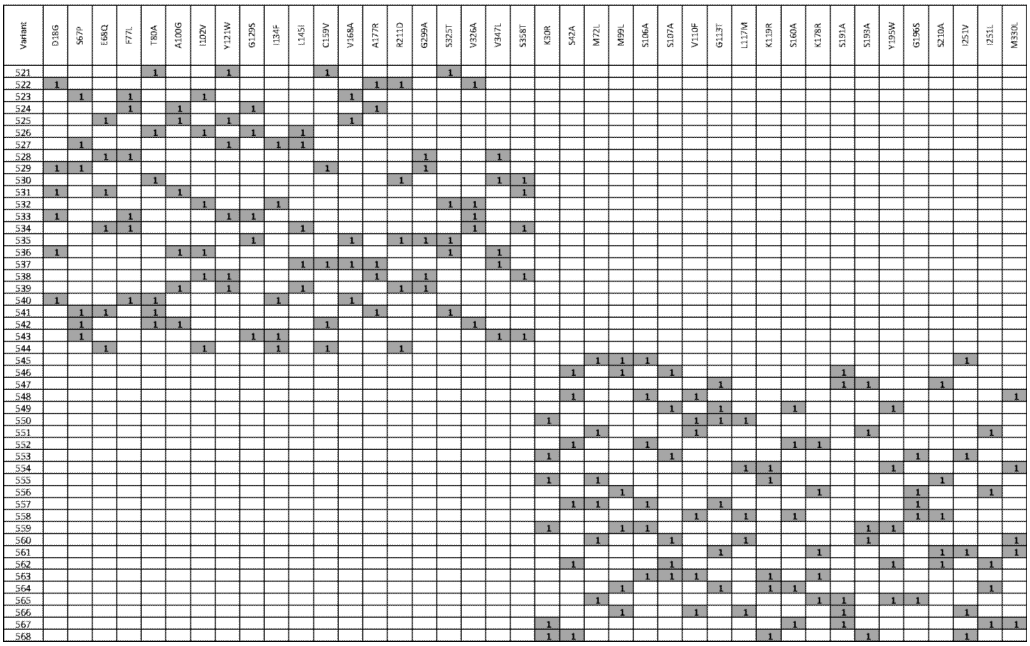

Variant	D18G	S67P	E68Q	F77L	T80A	A100G	I102V	Y121W	G129S	I134F	L145I	C159W	V168A	A177R	R211D	G229A	S325T	V326A	V347L	S363T	K30R	S42A	M72L	M99L	S106A	S107A	V110F	G113T	L127M	K139R	S160A	K178R	S191A	S193A	Y195W	G196S	S210A	I251V	I251L	M330L
521					1			1				1					1																								
522	1													1	1			1																								
523		1		1			1						1																												
524				1		1			1					1																												
525			1			1		1					1																												
526					1		1		1		1																														
527		1						1		1	1																														
528			1	1													1			1																				
529	1	1										1					1																								
530					1											1				1	1																				
531	1		1			1															1																				
532							1			1								1	1																						
533	1			1				1	1										1																						
534			1	1							1								1		1																				
535									1				1		1	1	1																								
536	1					1	1										1			1																				
537											1	1	1	1						1																				
538							1	1						1		1					1																				
539						1		1			1				1	1																									
540	1			1	1					1			1																											
541		1	1		1									1			1																							
542		1			1	1						1						1																						
543		1							1	1										1	1																				
544			1				1			1		1				1																									
545																							1	1	1														1		
546																						1		1		1								1							
547																												1						1	1			1			
548																						1			1		1		1												1
549																										1		1			1					1					
550																					1						1	1	1												
551																							1				1								1						1
552																						1			1							1	1							
553																					1					1										1		1			
554																													1	1					1					1
555																					1		1							1							1			
556																								1								1				1			1	
557																						1	1		1				1							1				
558																											1			1		1				1	1			
559																					1				1	1					1			1	1					
560																							1				1			1				1						1
561																												1				1			1	1			1
562																						1				1									1		1		1	
563																									1	1	1			1		1								
564																								1				1			1	1							1	
565																						1											1	1		1	1			
566																								1				1		1			1					1		
567																					1											1			1				1	1
568																					1	1									1				1			1		

(B)

Variant Set 1		Variant Set 2	
Identity	**Product Profile**	**Identity**	**Product Profile**
521	TW94b/TW94c/TW94d	545	TW94b/TW94c/TW94d
522	TW94b/TW94c/TW94d	546	TW94b/TW94c/TW94d
523	TW94b/TW94c/TW94d	547	Null
524	TW94b/TW94c/TW94d	548	TW94b/TW94c/TW94d
525	TW94b/TW94c/TW94d	549	Null
526	TW94b/TW94c/TW94d	550	Null
527	Null	551	TW94b/TW94c/TW94d
528	TW94b/TW94c/TW94d	552	TW94b/TW94c/TW94d
529	TW94b/TW94c/TW94d	553	TW94b/TW94c/TW94d
530	TW94b/TW94c/TW94d	554	TW94b/TW94c/TW94d
531	TW94b/TW94c/TW94d	555	TW94b/TW94c/TW94d
532	Null	556	TW94b/TW94c/TW94d
533	Null	557	Null
534	TW94b/TW94c/TW94d	558	TW94b/TW94c/TW94d
535	TW94b/TW94c/TW94d	559	TW94b/TW94c/TW94d
536	TW94b/TW94c/TW94d	560	TW94b/TW94c/TW94d
537	TW94b/TW94c/TW94d	561	Null
538	TW94b/TW94c/TW94d	562	TW94b/TW94c/TW94d
539	TW94b/TW94c/TW94d	563	TW94b/TW94c/TW94d
540	Null	564	Null
541	TW94b/TW94c/TW94d	565	TW94b/TW94c/TW94d
542	TW94b/TW94c/TW94d	566	TW94b/TW94c/TW94d
543	Null	567	TW94b/TW94c/TW94d
544	Null	568	TW94b/TW94c/TW94d